STOCHASTIC AND NON-STOCHASTIC EXPLICIT ALGEBRAIC MODELS FOR LES

A. Rasam†, G. Brethouwer, S. Wallin & A.V. Johansson
Linné FLOW Centre, Department of Mechanics,
Royal Institute of Technology
SE-10044 Stockholm, Sweden
†rasam@mech.kth.se

ABSTRACT

This paper consists of three parts. In the first part, we demonstrate the performance of the explicit algebraic (EA) subgrid-scale (SGS) stress model at $Re_\tau = 934$ and $Re_\tau = 2003$, based on friction velocity and channel half-width, for the case of large eddy simulation (LES) of turbulent channel flow. Performance of the EA model is compared to that of the dynamic Smagorinsky (DS) model for four different coarse resolutions and statistics are compared to the DNS of del Álamo & Jiménez (2003) and Hoyas & Jiménez (2008). Mean velocity profiles and Reynolds stresses are presented for the different cases. The EA model predictions are found to be reasonably close to the DNS profiles at all resolutions, while the DS model predictions are only in agreement at the finest resolution. The EA model predictions are found to be less resolution dependent than those with the DS model at both Reynolds numbers.

In the second and third parts, we use Langevin stochastic differential equations to extend the EA model with stochastic contributions for SGS stresses and scalar fluxes. LES of turbulent channel flow at $Re_\tau = 590$, including a passive scalar, is carried out using the stochastic EA (SEA) models and the results are compared to the EA model predictions as well as DNS data. Investigations, show that the SEA model provides for a reasonable amount of backscatter of energy both for velocity and scalar, while the EA models do not provide for backscatter. The SEA model also improves the variance and length-scale of the SGS dissipation for velocity and scalar. However, the resolved statistics like the mean velocity, temperature, Reynolds stresses and scalar fluxes are hardly affected by the inclusion of the stochastic terms.

INTRODUCTION

The recent study by Rasam *et al.* (2011) indicates that accuracy of LES of wall-bounded flows using isotropic eddy-viscosity-type models, strongly depends on the grid resolution. Nonlinear models which improve LES results at coarse resolutions, in comparison with the former models, would make LES computationally less expensive. The EA SGS stress model is a nonlinear model which has recently been introduced by Marstorp *et al.* (2009). The model uses an explicit algebraic solution of the transport equations of the anisotropy of SGS stresses. The first part of this study extends the earlier investigation of Rasam *et al.* (2011) to a higher Reynolds number. The performance of the EA model is compared to the DS model for different resolutions and two Reynolds numbers,

Improvements in LES predictions using stochastic modeling has been reported in several early studies, e.g. Schumann (1995). Langevin equations have been used for stochastic modeling in turbulent flows, see e.g. Marstorp *et al.* (2007). In the second part, the EA model is extended using a stochastic model based on the Langevin equations.

PART I: PERFORMANCE ANALYSIS OF THE EA MODEL

In this part, the performance of the EA and the DS models are compared in LES of channel flow at coarse resolutions. Simulations are carried out using a pseudo-spectral Navier–Stokes solver for incompressible flows. The code uses Fourier and Chebychev representations in the homogeneous and wall-normal directions, respectively. LES are carried out with a constant mass flux equal to the DNS values corresponding to $Re_\tau = 934$ and $Re_\tau = 2003$. A summary of the simulations is shown in table 1. The EA and DS SGS models are used in the simulations and are briefly described.

The EA model uses the following formulation for the SGS stress tensor τ_{ij}:

$$\tau_{ij} = K^{SGS}\left[\frac{2}{3}\delta_{ij} + \beta_1\tau^*\tilde{S}_{ij} + \beta_4\tau^{*2}\left(\tilde{S}_{ik}\tilde{\Omega}_{kj} - \tilde{\Omega}_{ik}\tilde{S}_{kj}\right)\right] \quad (1)$$

The model contribution consists of three parts: an isotropic part (the first term on the right-hand side, RHS), an eddy viscosity part (the second term on the RHS) and a nonlinear part (the last term on the RHS) which generates proper anisotropy. The filtered strain- and rotation-rate tensors are denoted by $\tilde{S}$ and $\tilde{\Omega}$, respectively, and τ^* is the time scale of the SGS motions. The model parameters β_1 and β_4 are functions of $\tilde{\Omega}$ and τ^*, see Marstorp *et al.* (2009). The SGS kinetic energy, K^{SGS},

Table 1. Summary of simulations for part I. Δx^+ and Δz^+ are streamwise and spanwise resolutions in wall units in physical space, respectively. The number of points in the wall-normal direction is N_y. L_x, L_z and $2h$ are the domain sizes in streamwise, spanwise and wall-normal directions, respectively.

Case	SGS model	Re_τ	L_x/h	L_z/h	Δx^+	Δz^+	N_y
EA1R1		938.7	8π	3π	184.3	92.2	97
EA2R1		951.0	8π	3π	124.6	62.3	97
EA3R1		966.0	8π	3π	94.9	47.4	129
EA4R1	Explicit	946.0	8π	3π	74.3	27.9	129
EA1R2	algebraic	2012	8π	3π	197.5	98.8	193
EA2R2		2031	8π	3π	133.0	66.5	257
EA3R2		2070	8π	3π	101.6	50.8	193
EA4R2		2031	8π	3π	79.8	30.5	257
DS1R1		828.7	8π	3π	162.7	81.4	97
DS2R1		873.5	8π	3π	114.3	57.2	97
DS3R1		896.5	8π	3π	88.0	44.0	129
DS4R1	Dynamic	912.8	8π	3π	71.7	26.9	129
DS1R2	Smagorinsky	1786	8π	3π	175.3	87.7	193
DS2R2		1876	8π	3π	122.8	61.4	257
DS3R2		1920	8π	3π	94.2	47.1	257
DS4R2		1958	8π	3π	76.9	28.8	257

and time scale, τ^*, are modeled as:

$$K^{SGS} = c\Delta^2|\widetilde{S}|^2, \quad \tau^* = \frac{36}{|\widetilde{S}|}\sqrt{c}, \tag{2}$$

where the coefficient c is determined dynamically using Germano's identity, Δ is the filter scale and $|\widetilde{S}| = \sqrt{2\widetilde{S}_{ij}\widetilde{S}_{ij}}$.

The DS model has an isotropic eddy viscosity description of the SGS stresses

$$\tau_{ij} - \frac{1}{3}\tau_{kk}\delta_{ij} = -2C_s\Delta^2|\widetilde{S}|\widetilde{S}_{ij}, \tag{3}$$

where C_s is determined dynamically using Germano's identity and δ_{ij} is the Kronecker delta.

RESULTS FOR PART I

Mean velocity profiles are shown in figure 1. The EA model predictions are in good agreement with the DNS profile at all resolutions for both Reynolds numbers. In contrast, the DS model predictions deviate from the DNS strongly at coarse resolutions and converge to the DNS gradually with increasing resolution. The EA model prediction of the mean velocity profiles is almost resolution independent for the current cases, while the DS model predictions vary considerably with resolution. Reynolds stresses are shown in figure 2(a)–(c). The DS model largely over-predicts the streamwise Reynolds stresses, R^+_{uu}, at coarse resolutions for both Reynolds numbers, see figure 2(a). In contrast, the EA model predictions are close to the DNS profile and the relative change in its predictions with increasing resolution is small. The DS model under-predicts R^+_{vv}

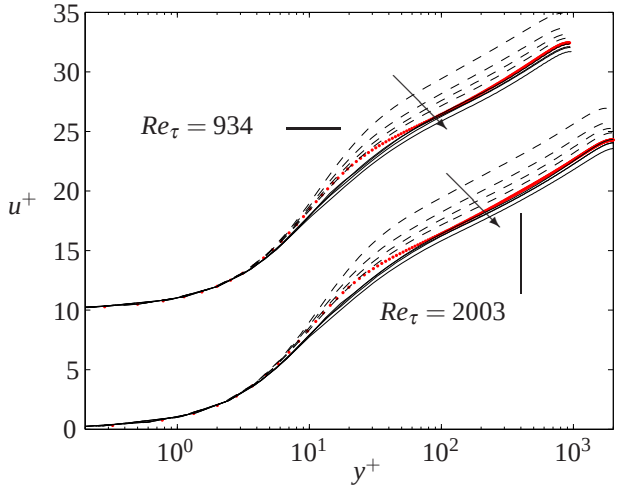

Figure 1. Mean velocity profiles in wall units. —— : EA model, – – : DS model and ··· : DNS. Profiles are shifted in the ordinate direction to separate the two Reynolds number predictions. Arrows point in the direction of increasing resolution.

and R^+_{ww}, see figures 2(b)–(c), while the EA model gives better predictions also for these components. Also, large variations in the DS model predictions, with increasing resolution, are observed for R^+_{vv} which is not observed in the EA model predictions. The better predictions of the EA model are attributed to its nonlinear formulation.

PART II: STOCHASTIC EA (SEA) SGS STRESS MODEL

We use the solution to the Langevin stochastic differential equation to introduce stochastic fluctuations in the instantaneous SGS stresses. This approach is similar to the one proposed in Marstorp *et al.* (2007) for stochastic formulation of the Smagorinsky model. The Langevin equation reads

$$d\mathscr{X}(x,t) = -a\mathscr{X}(x,t)dt + b\sqrt{2a}\,d\mathscr{W}(x,t), \tag{4}$$

or in the discretized form

$$\mathscr{X}(x,t+\Delta t) = (1-\frac{\Delta t}{\tau_{\mathscr{X}}})\mathscr{X}(x,t) + b\sqrt{\frac{2\Delta t}{\tau_{\mathscr{X}}}}\,d\mathscr{W}(x,t), \tag{5}$$

where Δt is the time step of the simulation, $a = 1/\tau_{\mathscr{X}}$, b is a constant and $dW(x,t)$ are spatially and temporally independent random numbers with zero mean and variance equal to one. The solution to the above Langevin equation is a statistically stationary process with zero mean and b^2 variance and a time scale $\tau_{\mathscr{X}}$. The SEA model is written as

$$a_{ij} = C_l\,(1+\mathscr{X}(x,t))\,\beta_1\tau^*\widetilde{S}_{ij} + \beta_4\tau^{*2}(\widetilde{S}_{ik}\widetilde{\Omega}_{kj} - \widetilde{\Omega}_{ik}\widetilde{S}_{kj}) \tag{6}$$

where C_l is a model constant and $a_{ij} = \tau_{ij}/K^{SGS} - 2/3\delta_{ij}$. The time scale of the stochastic process is estimated as

$$\tau_{\mathscr{L}} = C\left(\frac{\Delta^2}{\langle\Pi\rangle}\right)^{1/3}, \quad \Pi = -\tau_{ij}\widetilde{S}_{ij} = -\frac{\tau^*}{2}K^{SGS}\beta_1|\widetilde{S}|^2, \quad (7)$$

where $C = 1.5$ is a model constant, Π is the subgrid-scale dissipation and $\langle . \rangle$ denotes averaging in the homogenous directions.

In order to test the performance of the SEA SGS stress model, LES of channel flow at $Re_\tau = 590$ is carried out. A constant mass flux constraint is used in the simulations. A summary of the numerical simulations is given in table 2, see cases 1 and 3, and the results are compared to the EA model and DNS, see Rasam (2011).

Table 2. Summary of simulations for parts II and III. Δx^+ and Δz^+ are streamwise and spanwise resolutions in wall-units in physical space, respectively. The number of grid points in the wall-normal direction is N_y.

Case	SGS model	Re_τ	b	C_l	scalar	Δx^+	Δz^+	N_y
1	EA	584	–	–	×	57.3	28.7	65
2	EA	588	–	–	√	57.7	28.9	73
3	SEA	587	2.0	0.85	×	57.6	28.8	65
4†	SEA	588	2.0	–	√	57.7	28.9	73

† The EA model has been used for the SGS stresses.

RESULTS FOR PART II

Mean velocity profiles and Reynolds stresses are shown in figures 3(a)–(b). The EA model predictions are in good agreement with the DNS profiles both for mean velocity and Reynolds stresses. The SEA model predictions, case 3, are identical to the EA model predictions, case 1, which indicates that the stochastic formulation does not affect the low-order statistics of the resolved quantities. This is in agreement with the findings of Destefano *et al.* (2005). They show that the effect of the incoherent part of the SGS motions on the low-order statistics of a perfect LES would be negligible in the case of decaying isotropic turbulence. However, there have been other investigations that show improvements in the large-scale statistics using stochastic modeling, e.g. see Mason & Thompson (1992). All these investigations use the Smagorinsky model, where there are well-known problems in its formulation, e.g. see Marstorp *et al.* (2007). However, in the case of the EA model, large-scale statistics are already in good agreement with the DNS data. Therefore, improvements in those statistics are expected to be marginal. Nevertheless, the statistics of the energy transfer at the small scales are improved. In the following, we discuss some of these improvements.

The original EA model does not provide for backscatter of energy, Π^-, however, the SEA model provides for a reasonable amount of backscatter, see figure 4(b). The increase in forward scatter, Π^+, by the SEA model is equal to the amount of backscatter, see figure 4(a), therefore the total SGS dissipation, $\Pi^+ + \Pi^-$, is not changed by the SEA model. The root

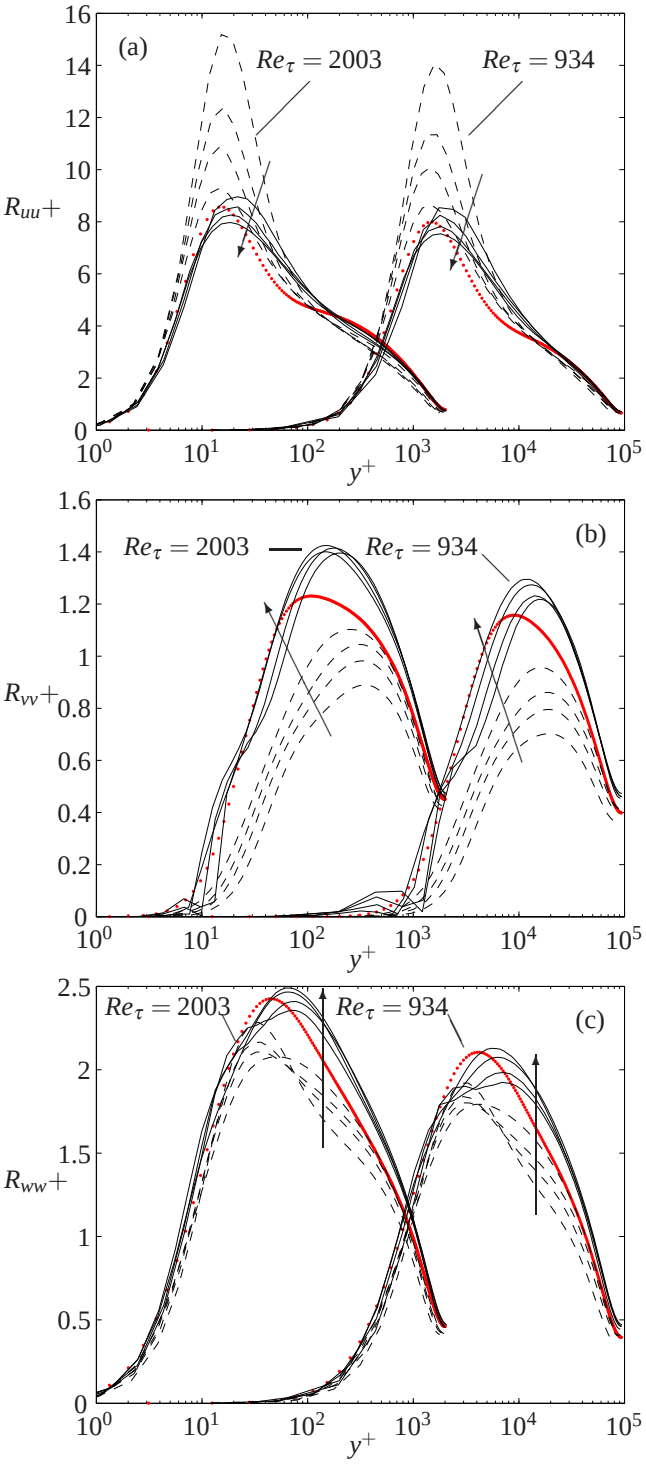

Figure 2. Resolved plus modeled (only for the EA model) Reynolds stresses in (a) streamwise R^+_{uu}, (b) wall-normal R^+_{vv} and (c) spanwise R^+_{ww} directions in wall units. —— : EA model, – – : DS model and ··· : DNS. Profiles are shifted in the abscissa direction to separate the two Reynolds number predictions. Arrows point in the direction of increasing resolution.

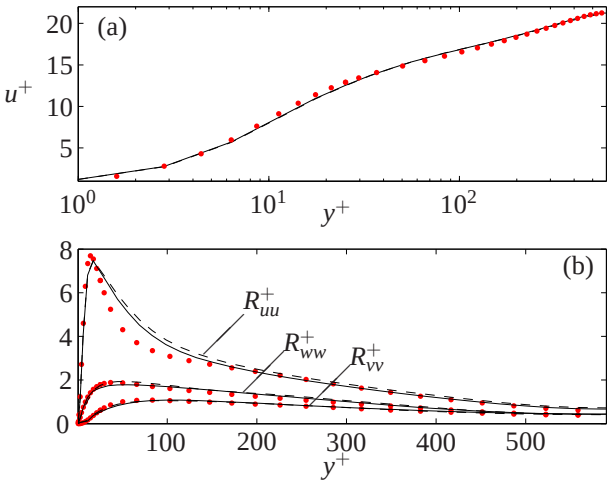

Figure 3. (a) Mean velocity profiles and (b) resolved plus modelled Reynolds stresses in wall units in streamwise, R^+_{uu}, spanwise, R^+_{ww}, and wall-normal, R^+_{vv}, directions —— : EA model (case 1), – – : SEA model (case 3) and ··· : DNS.

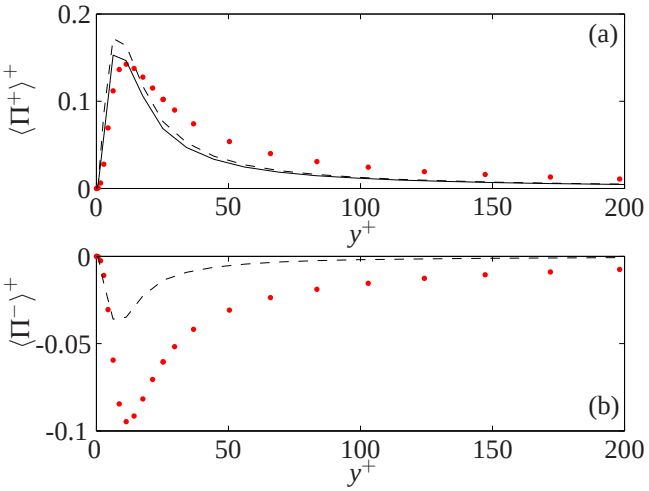

Figure 4. (a) Forward scatter and (b) backscatter for turbulent kinetic energy expressed in wall units. —— : EA model (case 1), – – : SEA mdoel (case 3) and ··· : DNS.

mean square of the SGS dissipation is shown in figure 5(a). The SEA model predicts larger values compared to the EA model and in better agreement with the DNS data, showing that the SGS dissipation becomes more intermittent.

Another quantity of interest is the length scale of the SGS dissipation which is obtained from the spatial two-point correlation of the SGS dissipation

$$L_x[\Pi] = \int_0^{\frac{1}{2}L_x} \frac{\langle \Pi'(x_0)\Pi'(x_0+x)\rangle}{\langle \Pi'^2 \rangle} dx, \tag{8}$$

where the upper integration limit is half the simulation box length, L_x, in the streamwise direction and Π' is the fluctuating part of Π. The SGS dissipation length scale computed from equation (8) is shown in figure 5(b), where it has been non-dimensionalized by the filter scale $\Delta = \sqrt[3]{\Delta x \langle \Delta y \rangle \Delta z}$, where

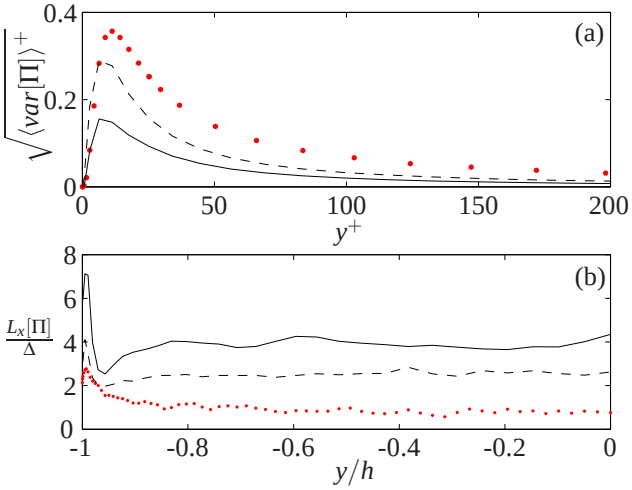

Figure 5. (a) Root mean square of SGS dissipation in wall units and (b) length scale L_x of the SGS dissipation normalized with the grid sale $\Delta = \sqrt[3]{\Delta_x \langle \Delta_y \rangle_{y-dir.} \Delta_z}$. —— : EA model (case 1), – – : SEA model (case 3) and ··· : DNS.

$\langle . \rangle$ denotes averaging of Δy in the wall-normal direction. The SGS dissipation length-scale computed from filtered DNS is slightly smaller than the mean filter scale, Δ, which emphasizes the fact that there is a large amount of spatially uncorrelated noise in the SGS dissipation leading to short correlation lengths. The prediction of the EA model is almost four times larger than the grid scale in most of the channel with larger values close to the wall, while there is a factor of two improvement using the SEA model. These results show that the length scales are reduced and the SGS dissipation becomes more intermittent by introducing the stochastic model.

PART III: STOCHASTIC EA SGS SCALAR FLUX MODEL

The EA SGS scalar flux model, see Rasam (2011), has the following formulation for the SGS scalar fluxes q_i :

$$q_i = -\tau^* A^{-1}_{ij} \tau_{jk} \frac{\partial \widetilde{\theta}}{\partial x_k}, \tag{9}$$

where τ^* is obtained from equation (2), τ_{jk} is the SGS stress tensor and

$$\mathbf{A^{-1}} = \frac{(G^2 - \frac{1}{2}Q_1)\mathbf{I} - G\tau^*(\tilde{\mathbf{S}} + \tilde{\mathbf{\Omega}}) + \tau^{*^2}(\tilde{\mathbf{S}} + \tilde{\mathbf{\Omega}})^2}{G^3 - \frac{1}{2}GQ_1 + \frac{1}{2}Q_2},$$

$$G = \frac{4.8K^{SGS}}{(0.2\Delta|\widetilde{S}|)^2} - \frac{1}{2r}, \quad r = 0.5,$$

$$Q_1 = \tau^{*^2} \mathrm{tr}\left(\widetilde{\mathbf{S}}^2 + \widetilde{\mathbf{\Omega}}^2\right), Q_2 = \frac{2}{3}\tau^{*^3} \mathrm{tr}\left(\widetilde{\mathbf{S}}^3\right) + 2\tau^{*^3} \mathrm{tr}\left(\widetilde{\mathbf{S}}\widetilde{\mathbf{\Omega}}^2\right),$$

where tr (.) denotes the trace of a matrix, boldface denotes tensors and $\mathbf{I}$ is the unity tensor. The EA model has the advantage, over all isotropic models based on eddy diffusivity assumption, that its predictions are not in general aligned with

the resolved scalar gradient, see Rasam (2011). The stochastic EA SGS scalar flux model is obtained from equation (9) in the same way as was done for the anisotropy of the SGS stresses

$$q_i = -\tau^* A_{ij}^{-1} \tau_{jk} \frac{\partial \widetilde{\theta}}{\partial x_k} \left(1 + \mathscr{X}(x,t)\right). \qquad (10)$$

RESULTS FOR PART III

In order to test the SEA SGS scalar flux model, LES of turbulent channel flow is carried out with a passive scalar (Pr=0.72). The channel walls are kept at constant but different temperatures. We use a constant mass flux constraint with the bulk Reynolds number equal to the corresponding DNS at $Re_\tau = 590$, see Rasam (2011). A summary of the simulation cases is given in table 2, see cases 2 and 4.

It was found that the large-scale statistics of velocity are not affected by the stochastic model. We have found the same to be true for the large-scale scalar statistics. The mean and root mean square (RMS) of the scalar are shown in figures 6(a)–(b). The predictions of the EA and SEA models are identical and compare well with the corresponding DNS profiles. The scalar fluxes, $\langle u'\theta' \rangle$ and $\langle v'\theta' \rangle$, are shown in

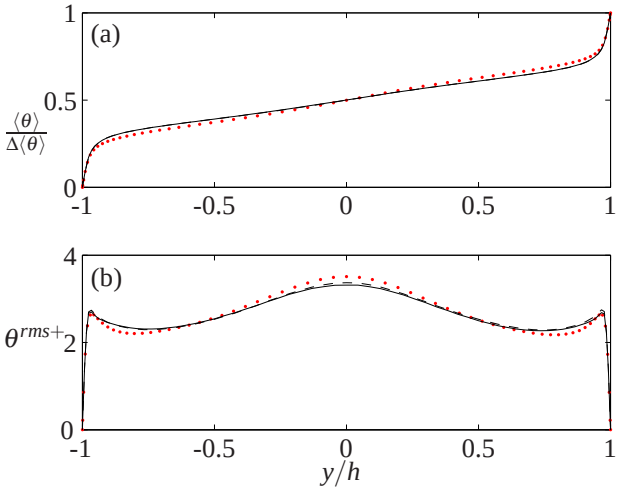

Figure 6. (a) Mean temperature, $\langle\theta\rangle$, normalized with the mean temperature difference, $\Delta\langle\theta\rangle$, and (b) root mean square of temperature θ^{rms} normalized with $\frac{\nu}{Pru_\tau}\left|\left\langle\frac{\partial\langle\theta\rangle}{\partial y}\right\rangle\right|_{wall}$. —— : EA model (case 2), – – : SEA model (case 4) and ··· : DNS.

figures 7(a)–(b). A close correspondence with the DNS profile exists and the two models give identical results. The SGS dissipation of the scalar variance for the SEA model is

$$\chi = (1 + \mathscr{X})\tau^* A_{ij}^{-1} \tau_{jk} \frac{\partial \widetilde{\theta}}{\partial x_k} \frac{\partial \widetilde{\theta}}{\partial x_i}, \qquad (11)$$

which can be further split into $\chi = \chi^+ + \chi^-$. Here χ^+ and χ^- are the forward- and backscatter of the SGS dissipation of

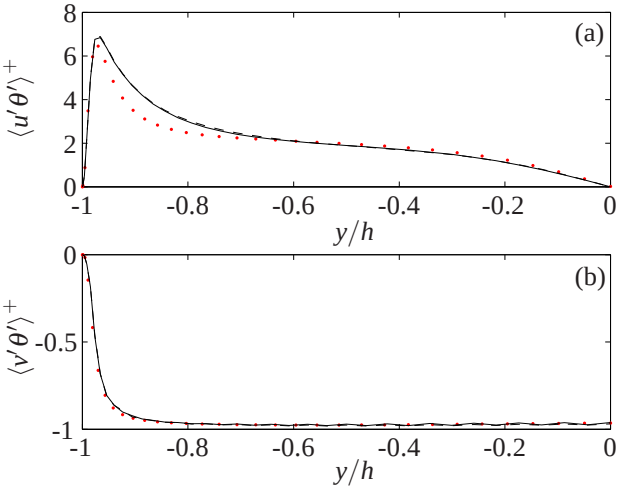

Figure 7. Resolved plus modeled turbulence scalar fluxes in (a) streamwise, $\langle u'\theta' \rangle$, and (b) wall-normal, $\langle v'\theta' \rangle$, directions normalized with $\frac{\nu}{Pru_\tau}\left|\left\langle\frac{\partial\langle\theta\rangle}{\partial y}\right\rangle\right|_{wall}$. —— : EA model (case 2), – – : SEA model(case 4) and ··· : DNS.

scalar variance, respectively. They are shown in figures 8(a)–(b). The SEA model predicts slightly larger than half the backscatter computed from filtered DNS. Its predictions of the forward scatter also give considerable improvements in comparison with the EA model and practically matches the filtered DNS data. The variance of the SGS dissipation is significantly

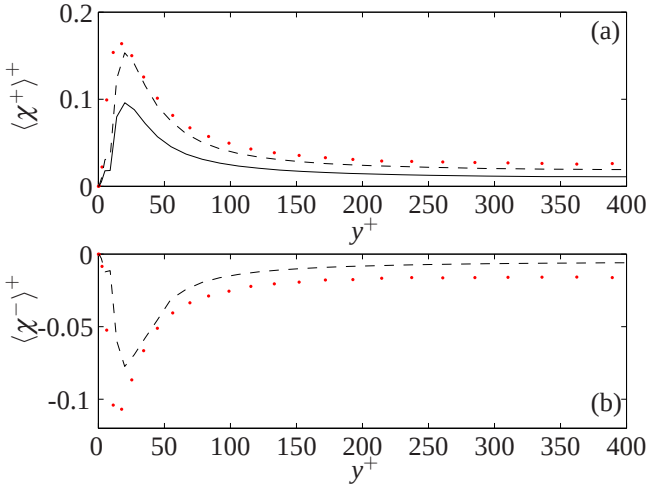

Figure 8. (a) Forward scatter and (b) backscatter for scalar variance dissipation, expressed in wall units. —— : EA model (case 2), – – : SEA model (case 4) and ··· : DNS.

improved by the stochastic model, see figure 9(a), which reflects the improvement in the intermittency of the SGS dissipation. The length scale of the subgrid-scale dissipation for the scalar variance is computed as

$$L_x[\chi] = \int_0^{\frac{1}{2}L_x} \frac{\langle \chi'(x_0)\chi'(x_0+x)\rangle}{\langle \chi'^2 \rangle} dx. \qquad (12)$$

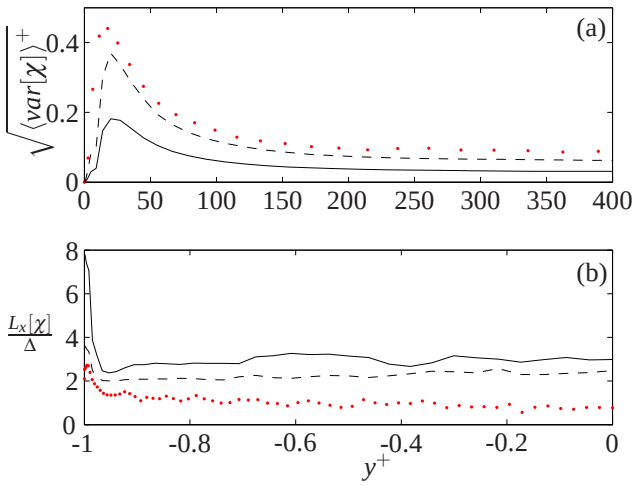

Figure 9. (a) Root mean square of SGS dissipation variance for the scalar expressed in wall units and (b) length scale, L_x, of the SGS dissipation of the scalar variance normalized with the grid sale, $\Delta = \sqrt[3]{\Delta_x \langle \Delta_y \rangle_{y-dir.} \Delta_z}$. ——: EA model (case 2), – – : SEA model (case 4) and ···: DNS.

The SGS dissipation length scale is shown in figure 9(b). The general behavior of the SGS dissipation length scale for scalar variance and turbulent kinetic energy is the same. Accordingly, the length scale computed from filtered DNS is smaller than the mean filter scale Δ, which also indicates the fact that the amount of spatially uncorrelated noise in the SGS scalar fluxes is large. The prediction of the EA model is almost three times larger than the grid scale, while there is a notable amount of improvement using the SEA model in the outer region and close to the wall.

CONCLUSIONS

LES of channel flow at four different resolutions, ranging from coarse to medium, were carried out at two Reynolds numbers $Re_\tau = 934$ and $Re_\tau = 2003$. It was found that the EA model predictions were close to the DNS profile at all resolutions. Its predictions of the mean velocity were almost independent of resolution for the two Reynolds numbers and its predictions of the Reynolds stresses showed a small variation with increasing resolution. In contrast, the DS model largely over-predicted the mean velocity and streamwise Reynolds stresses at coarse resolutions for both Reynolds numbers. The DS model predictions converged to the DNS profile with increasing resolution but they showed large variations with resolution. In conclusion, LES using the EA model leads to more accurate results, for mean velocity and Reynolds stresses, at less computational cost.

In the second part, the stochastic model of Marstorp *et al.* (2007) has been used to introduce random fluctuations in the EA SGS stress model of Marstorp *et al.* (2009) and the EA SGS scalar flux model of Rasam (2011). LES of turbulent channel flow at $Re_\tau = 590$ is carried out including a passive scalar (temperature) to validate the new models. The large-scale quantities are very well predicted by the EA models without the stochastic extensions. Inclusion of the stochastic process does not further improve those statistics in a accordance with the results of Destefano *et al.* (2005). The main part of this study was focused on the statistics of SGS dissipation, for both the velocity and scalar fields. It was found that the stochastic explicit algebraic (SEA) model can provide for a reasonable amount of backscatter of energy both for turbulent kinetic energy and the scalar variance. The variance of the SGS dissipation is also improved in both cases, showing a more realistic level of intermittency of the SGS dissipation. The length scales of the SGS dissipation were reduced by the SEA model in comparison with the EA model and in better agreement with the DNS, showing that the incoherent part of the SGS dissipation is increased. The findings reported here, are important in the sense that they show that stochastic models improve different aspects of the SGS energy transfer. This is important in cases where the small-scale statistics are of prime importance, e.g. see Pitsch (2006).

ACKNOWLEDGMENTS

We thank Dr. O. Grundestam for his contributions to this work. Support from the Swedish research council through grant numbers 621-2010-6965 and 621-2007-4232 and computer time provided by the Swedish National Infrastructure for Computing (SNIC) is gratefully acknowledged.

REFERENCES

del Álamo, J. C. & Jiménez, J. 2003 Spectra of the very large anisotropic scales in turbulent channels. *Phys. Fluids* **15** (6), L41–L44.

Destefano, G., Goldstein, D. E. & Vasilyev, O. V. 2005 On the role of subgrid-scale coherent modes in large-eddy simulation. *J. Fluid Mech.* **525**, 263–274.

Hoyas, S. & Jiménez, J. 2008 Reynolds number effects on the Reynolds-stress budgets in turbulent channels. *Phys. Fluids* **20** (101511).

Marstorp, L., Brethouwer, G., Grundestam, O. & Johansson, A. V. 2009 Explicit algebraic subgrid stress models with application to rotating channel flow. *J. Fluid. Mech.* **639**, 403–432.

Marstorp, L., Brethouwer, G. & Johansson, A. V. 2007 A stochastic subgrid model with application to turbulent flow and scalar mixing. *Phys. Fluids* **19** (035107).

Mason, P. J. & Thompson, D. J. 1992 Stochastic backscatter in large-eddy simulations of boundary layers. *J. Fluid Mech.* **242**, 51–78.

Pitsch, H. 2006 Large-eddy simulation of turbulent combustion. *Annu. Rev. Fluid Mech.* **38**, 453–482.

Rasam, A. 2011 *Explicit algebraic subgrid-scale stress and passive scalar flux modeling in large eddy simulation*, pp. 61–80. Licentiate thesis, Trita-MEK 2011:05, Royal institute of technology, Stockholm, Sweden.

Rasam, A., Brethouwer, G., Schlatter, P., Li, Q. & Johansson, A. V. 2011 Effects of modelling, resolution and anisotropy of subgrid-scales on large eddy simulations of channel flow. *J. Turbulence* **12** (10), 1–20.

Schumann, U. 1995 Stochastic backscatter of turbulence energy and scalar variance by random subgrid-scale fluxes. *Proc. R. Soc. Lond. A* **451**, 293–318.